THE SUPERCONDUCTING MAGNET FOR THE
BROOKHAVEN NATIONAL LABORATORY 7-FOOT BUBBLE CHAMBER*

D.P. Brown, R.W. Burgess, and G.T. Mulholland
Brookhaven National Laboratory
Upton, New York

INTRODUCTION

An air core, fully stabilized superconducting magnet has been constructed for the Brookhaven National Laboratory 7-Foot Bubble Chamber. The magnet incorporates conductor face cooling and stainless-steel reinforcement in an effort to maximize the performance-cost ratio. The design approach is integral with that of the Bubble Chamber. The conductor selection, the magnet design, construction considerations, cryogenic support facilities, and preliminary test results are described.

THE MAGNET

The magnet[1] has 16 double layers, or pancakes, wound with a conductor consisting of six NbTi (48% Ti by volume) cores metallurgically bonded to, and evenly distributed within a 2 in. $\times$ 0.078 in. OFHC[†] copper substrate. Each turn contains four strips: the stabilized superconductor, a Mylar insulator, a stainless-steel strength member, and a copper cooling channel spacer, in that order radially outward (Fig. 1). The double wound layers are arranged in two stacks in an annular helium Dewar concentric with the chamber's vertical axis. The two stacks are separated from each other by a bridge structure to allow the entry of particle beams into the chamber (Fig. 2).

The layers are connected in series electrically and externally powered through gas-cooled leads by a conventional power supply. The central field expected is 30 kG at 6000 A (see Table I).

CONDUCTOR SELECTION AND TEST RESULTS

Preliminary investigations indicated that the minimum superconductor current density expected in the processed composite conductor (actual 4.3×10^4 A/cm^2) was an order of magnitude higher than the composite conductor current density (actual 6×10^3 A/cm^2) required, allowing thermal and stress considerations to proceed without detailed consideration of the superconductor but assuming a reasonable distribution of superconductor in the copper and good thermal and mechanical contact.

If the copper, by virtue of its own strength or in combination with the strength of a reinforcing strip, can support the forces involved without significant resistivity change, the full stability criterion can be written as:

---

1. D.A. Kassner, in International Colloquium on Bubble Chambers, Heidelberg, 1967, (Yellow Report CERN 67-26), p. 435.

TABLE I

7-Foot Bubble Chamber Magnet Parameters

Number of double pancakes	16
Total number of layers	32
Turns per layer	44
Total number of turns	1408
Coil current (A)	6000
Central field (kG)	30
Maximum vertical field (kG)	40.5
Maximum radial field (kG)	27.9
Coil inside diameter (in.)	94.6
Coil outside diameter (in.)	108.4
Conductor length per layer (ft)	1160
Total conductor length (ft)	37 200
Weight per pancake (lb)	2000
Total coil weight (lb)	41 000
Inductance (H)	4
Energy (MJ)	72

$$I = \left(\frac{\eta k t_c t_s h^{3/2}}{\rho(H_{max})} \right)^{\frac{1}{2}} \quad , \tag{1a}$$

$$J \cong \frac{h^{-\frac{1}{4}}}{(t_c + t_s)} \left(\frac{\eta k t_c t_s}{\rho(H_{max})} \right)^{\frac{1}{2}} \quad , \tag{1b}$$

where I is the fully stable current (A), η is the normalized surface exposure and flow efficiency parameter (0.5, here), k is the critical heat flux proportionality constant[2] (6 W/cm$^{5/2}$, in the region of interest), t_c is the thickness of copper (cm), t_s is the thickness of cooling channel (cm), h is the channel and conductor height (cm), $\rho(H_{max})$ is the resistivity at the highest field within the coil ($\Omega \cdot$cm) [resistance ratio at H = 0, $\rho(300°K)/\rho(4°K) = 200$], and J is the average current density (A/cm^2).

The product term $\sqrt{t_c t_s}$ causes a rather flat current density maximum at $t_s = t_c$, allowing t_c to be increased (decreased) as t_s is decreased (increased) for reasons of strength (economics) with little effect on J.*

---

* J actual = 2.5×10^3 A/cm^2.

2. M.N. Wilson, in Pure and Applied Cryogenics (Pergamon Press, 1966), Vol. 6, p. 109.

The maximum heat flux with all the current in the copper is 0.34 W/cm^2. This number is in good agreement with the demonstrated stability of the Maddox and Taylor magnet[3] at 0.4 W/cm^2 with similar cooling provisions.

A stress analysis[4] taking into account (1) the nonlinear stress-strain relationship for copper, (2) the addition of an elastic reinforcing material, (3) the details of radial and axial support, and (4) the thermal contraction differences, was used as the basis for a computer study[5] of the stress distribution within the coil. The results of the study indicated that a stainless-steel strip 0.012 in. thick was sufficient to reinforce the 0.078 in. copper at the maximum (full field) load.

The important features of the reinforcement approach (the layers are tightly wound) taken here are: (1) the copper, required by the stability considerations, is used to its yield strength, (2) each turn transfers the stress in excess of that consistent with the mean layer strain to the next outer turn, until (3) the strength required of each turn is very nearly equal, resulting in minimum composite conductor and stainless steel material requirements. Note that here the stainless steel does not support the major portion of the (hoop) forces but guards against what at room (or higher) temperatures would be called "creep" in the copper.

The maximum stresses in the copper and stainless steel at 30 kG are 16.0 and 38.5 kpsi, respectively. The thermal stresses, which account for 1.25 kpsi in the copper and 6.7 kpsi in the stainless steel (Fig. 3),* are given by:

$$\sigma_1 = \frac{[\int (\pm \Delta T) dT] E_1 t_2}{(E_1/E_2) t_1 + t_2} \quad , \tag{2}$$

where E = elastic modulus, t = radial thickness, ΔT = differential thermal expansion coefficient, T = temperature, and subscripts 1 and 2 refer to copper and stainless steel, or vice versa. Using the fact that most of the stress is hoop stress and that the calculation takes the circumferential conductor and reinforcement strains equal, the "effective" elastic modulus of the copper is less than

$$\bar{E}_c < \frac{(16.0 - 1.25) \; 28 \times 10^3 \; kpsi}{(38.5 + 6.7)} = 9.2 \times 10^3 \; kpsi \; .$$

It is interesting to note that the superconductor, with a modulus of $\sim$ 13 $\times$ 10^3 kpsi, and 115 kpsi ultimate tensile strength, can lend some of its strength to the mechanical composite. The superconductor strength and a conservative approximation to the copper stress-strain relationship serve as the design margin.

The selection of stainless steel as the reinforcement material in this application is not to imply that it is the best material as the thickness of reinforcement approaches that of the composite conductor in larger diameter magnets of equal field (at the coil) and current density. In fact, Eq. (2) suggests that a copper alloy

---

*The differences between the quoted stresses and those implied by Fig. 3 are radial and axial copper bending stresses.

3. B.J. Maddock et al., in Proc. 2nd Intern. Conf. Magnet Technology, Oxford, 1967, p. 533.

4. R.P. Shutt, Brookhaven National Laboratory Internal Notes (1966).

5. S. Kern, Brookhaven National Laboratory Program MAGIC (1966).

(e.g. BeCu, or phosphor bronze) may be a better choice with the nonlinear stress-strain relationship of the copper affording the stress transfer mechanism.

The test results obtained in the Brookhaven 8-in. bore 60-kG superconducting magnet test facility[6] on the composite conductor, which was manufactured[7] to a conservative 4000 A — 20 kG central field specification (the original design), indicated that the conductor would actually perform to critical currents consistent with central fields of 24 to 28 kG. The composite conductor exhibited a 5:1 critical current anisotropy favoring the vertical field component, so that the region of highest radial field, and not that of the highest total field, within the coil determined the limiting condition. In an effort to maximize the ratio of central field to maximum radial field by redistribution of the conductors at the extremes of the magnet coil, various coil configurations were studied. Construction details and helium Dewar constraints limited the possibilities to the 9% increase of Fig. 4b. The ratio change increased the predicted central field value to between 25.4 and 29.7 kG. By selecting conductor lengths with the higher critical current values for magnet pancakes in the higher field regions, the upper magnetic field limit may be achieved.

CONDUCTOR MECHANICAL CONSIDERATIONS

The composite superconductor material contains six niobium-titanium cores, each with a cross-sectional area of approximately 0.00375 sq.in., arranged in the copper conductor as shown in Fig. 1. Polished and etched sections examined under X 500 magnification (see Fig. 5) demonstrated that the bonding was sound and free of voids. Short pieces were acid etched on one side to expose three NbTi cores. The cores were gripped at one end and peeled away from the copper. The break occurred in the copper and not at the Cu-NbTi interface.

When copper and NbTi are metallurgically bonded, the composite material exhibits a higher tensile strength than copper alone, and a higher ultimate elongation than NbTi alone, as illustrated in Figs. 6 and 7. The copper supports the NbTi cores to the extent that the NbTi has an increase of approximately 25% in its elastic limit. This can be seen from the difference in strain to the apparent yield points in the curves in Figs. 6 and 7. X-ray photographs of a fractured specimen of the composite material showed that each NbTi core had yielded and fractured in succession at a number of places.

MAGNET CONSTRUCTION

A top and a bottom layer, each of 44 turns, are wound to make a double "pancake" assembly. The inside ends of the conductor are electrically connected and mechanically clamped to a curved plate at the inside diameter (Fig. 9). This allows the interpancake electrical connections to be made on the (exposed) outside diameter of the assembly. Open phenolic insulating spacers of 0.125 and 0.625 in. thicknesses separate the layers and pancakes, respectively, to allow the radial and axial flow of liquid helium (Fig. 8). The 0.625 in. spacers are assemblies of 0.75 in. wide blocks, spaced 1.5 in. on center by tubular spacers mounted on 0.125 in. phosphor bronze connecting rods.

6. J.A. Bamberger et al., in Advances in Cryogenic Engineering (Plenum Press, 1968), Vol. 13, p. 132.

7. J. Wong et al., J. Appl. Phys. 39, 2518 (1968).

In the double-layer winding procedure the inside ends of the composite superconductor strips are soldered to the crossover plate and clamped along with the Mylar-backed stainless-steel strip. The strips are formed around the ends of the crossover plate with a cuff made from a short length of composite superconductor soldered at the inner diameter to compensate for the reduction in critical current caused by the sharp bend. The plate is then mounted to a mandrel on the winding table. The table is rotated by a geared, constant torque, variable speed air motor.

The lower layer is wound with the upper coil supply reels of superconductor and Mylar-backed stainless-steel strip riding at the center of the table. The copper cooling spacer strip is fed in so that all three strips are wound simultaneously. After 44 turns are wound the ends of the strips are clamped to the table and the excess cut off. The upper layer supply reels that were riding at the center of the winding table are now placed on the supply tables (adjusted to the new level), the 0.125 in. insulating spacers are positioned on the lower layer, and the upper layer is wound in counter rotation. Two aluminum bronze electrical connector backing plates (Fig. 10) are sandwiched in the last turn of each layer in positions that vary from one double pancake to the next to offset alternately the radial clamps, and to comply with the arrangement of electrical connections (Fig. 14).

A fiberglass end clamp is then fixed in position between the upper and lower conductor ends, and the ends are formed around it and secured with bolted clamping plates (Fig. 11). The end clamp restrains the hoop forces transferred to the outer turns of the coil, causing each conductor end to pull against the other.

When the twelve radial clamps (Fig. 12) are secured to the coil, the double layer assembly is complete (Fig. 13). Eight double layers are stacked, with interleaved 0.625 in. spacers, on a stainless-steel bottom washer, and the whole assembly is tied together by 0.625 in. diameter 7075-T6 aluminum rods to a stainless-steel top washer. The top washer of the lower magnet half has upward protruding threaded studs to form, together with a T-section, an I-section stainless-steel "bridge" structure which separates the lower and upper magnet halves. The upper coils are similarly stacked on the T-section structure, and tied with aluminum rods to a top washer.

The bolts that fasten the magnet to the Dewar base and the aluminum tie rods must withstand the 2g dynamic loading (82 klb) associated with the bubble chamber expansion. The tie rods are pre-tensioned, because of this dynamic loading, with Preload Indicating Washers to assure that the stack is held tightly. Aluminum, rather than stainless steel, was chosen as the tie rod material as it has a higher thermal contraction than the copper-phenolic combination and acts as a thermal compensator on cooldown, reducing the necessary room temperature pre-tension to 48 kpsi. The maximum vertical loads due to the magnetic forces occur at approximately 1/3 the magnet half height, measured above and below the beam bridge, and are directed toward the center. At 30 kG this corresponds to a compressive stress of 10.3 kpsi in the copper of the conductor at the 0.75 in. wide phenolic spacers. The pitch of the phenolic insulating spacers is a compromise between the open space necessary for free liquid helium flow and a reasonable stress level.

When both halves of the magnet are placed in the Dewar and secured, parallel composite superconductor electrical inter-pancake jumper strips are temperature control soldered and clamped in place. The arrangement (Fig. 14) was designed to give the jumper strips sufficient length so they could be bowed to allow the flexibility required by the sum of the copper and phenolic spacer thermal contractions.

DESCRIPTION OF DEWAR, REFRIGERATOR AND PLUMBING

The magnet Dewar is an annular vessel of type 316L stainless steel that fits closely around the magnet and shares a common vacuum tank with the bubble chamber. Approximately 3000 liters of liquid helium are required to fill the vessel with the magnet in place.

The Dewar is supported by three legs which rest on pads cooled with liquid hydrogen. The legs are designed on the basis of a vibrational analysis of deflections and forces on the magnet during the bubble chamber expansion cycle, and leg deflection due to contraction of the Dewar relative to its room temperature supports. These considerations have made it necessary to use a leg cross section which is heavier than that required to support the weight of the magnet and Dewar in the static situation. The hydrogen cooling of the legs, however, provides a means of reducing conduction losses to the helium Dewar to a low value.

Each of the cylinders which form the walls of this vessel have cooling loops on the vacuum side. The coolant passes through 0.75 in. o.d. tubing that has been tack-welded and soft-soldered to the walls. The loops are provided for precooling the magnet with liquid nitrogen and liquid hydrogen while pressurizing the magnet Dewar with helium gas, thus eliminating the necessity of purging the main Dewar volume at low temperatures.

Originally the magnet current leads were helium gas cooled. Each lead was constructed of 76 parallel 0.125 in. o.d. copper tubes soldered into terminal blocks at both ends. The gas flow was inside of the tubes. Each lead was about 0.75 in.^{2} in cross section and 36 in. in length. The leads were extrapolated from leads used to supply the current for the short sample test program described earlier. The test leads had an optimum at 2900 A, but were used for short periods of time at 6000 A.

The Dewar was insulated only with NRC-2 aluminized Mylar insulation applied at a density of 100 layers per inch. Four inches of insulation are used in the vacuum space between room temperature and helium temperature. One inch of insulation is used in the vacuum space between hydrogen (bubble chamber) temperature and helium temperature.

The cooldown weight of the magnet and Dewar is about 53 klb. There are 14 tons of copper, 12 tons of stainless steel and 0.5 tons of plastics.

The helium refrigerator-liquefier used with the magnet is an ADL Model 2000 machine. It has a capacity of 60 liter/h as a liquefier, and 240 W at 4.5°K as a refrigerator. The machine uses liquid nitrogen precooling and has two 3 in. bore expansion engines. A non-lube three-stage Norwalk compressor supplies gas for the system.

The flow from the refrigerator goes to an intermediate supply Dewar and then to the magnet Dewar. A simplified schematic is shown in Fig. 15. The intermediate supply Dewar is used to insure a liquid helium supply for the magnet in the event of a refrigerator failure.

A schematic of the helium cooldown and fill system is shown in Fig. 16. During cooldown, liquid helium or cold gas is introduced at the bottom of the Dewar, directly under the magnet coils. The gas flows upward, enters the gas return piping, and can either be returned to the refrigerator or directly to compressor suction through a warm-up coil. When the Dewar has been filled, flow into the Dewar is directed to the top, instead of the bottom. The boil-off gas is returned to the refrigerator.

In addition to the vent and relief valves on the gas phase lines, two 1.5 in. liquid vent valves and a 6 in. rupture disk at the bottom of the Dewar provide protection against overpressure of the vessel.

TRIAL COOLDOWN

A trial cooldown of the magnet without the hydrogen bubble chamber was conducted from May 9 to June 2, 1968. Attempts to fill the Dewar with liquid helium were unsuccessful, but it was possible to run the magnet at 3300 A and 16.5 kG, in cold gas.

The magnet Dewar and refrigeration system were purged and liquid nitrogen precooling started on May 9. The magnet had reached a temperature of less than 100°K in about four days. It had not been planned to use a liquid hydrogen precool for this test, but because of the slow rate of cooling obtained with the helium liquefier, some plumbing changes were made and liquid hydrogen was circulated in the cooling loops on May 21. This cooled the magnet to about 30°K. A series of attempts were made to cool the magnet further with the refrigerator. It soon became apparent that the heat load exceeded the capacity of the refrigerator and that additional refrigeration in the form of purchased liquid would have to be used. A number of attempts were made to supply liquid from the refrigerator while at the same time maintaining flow from an outside Dewar. Because of plumbing limitations, the procedure was finally abandoned and an intermittent transfer operation was employed. This allowed the use of liquid at a rate in excess of liquefier capacity.

On May 25, the magnet was cooled to a temperature of 5 to 6°K when an interruption of the nitrogen flow due to a plugged supply Dewar caused a loss of refrigeration and leg cooling. The magnet warmed up and it was decided to interrupt the helium cooling flow in order to reliquefy all the helium gas in storage. The magnet was maintained at a temperature of 25°K with liquid hydrogen during this operation.

On June 1, the magnet was cooled to less than 5°K. Repeated attempts were made to fill the Dewar with liquid, using "bottom fill" mode, "top fill" mode and a combined "top-bottom fill" mode. No detectable amount of liquid was collected in the Dewar. By the morning of June 2, there was not enough liquid in storage to fill the Dewar. It was decided to attempt to run the magnet in cold gas. As the current was increased through 3300 A, the coil went normal causing the Dewar pressure to rise about 5 psi to 8 psig. The excess pressure was vented through the liquid dump valves. The magnet current had slowly decreased to 1500 A when the rest of the field energy was dumped into an external resistor. Strain gauges installed on the magnet showed no significant movement during the entire test.

A number of system modifications were indicated by these tests. Modifications which are to be included prior to the next cooldown are:

1) A hydrogen-cooled radiation shield using the effluent gas from the bubble chamber cooling loops as the coolant will be added.

2) The transfer lines will be liquid nitrogen shielded.

3) Hydrogen, instead of helium, gas will be used for power lead cooling. Because the helium refrigeration is supplied by a closed system, the gas used to cool the leads reduced the refrigeration available for other purposes by about 80 W.

4) A better system for utilization of purchased liquid in parallel with the refrigerator will be installed.

5) A bypass around the J-T heat exchanger of the refrigerator
   will be added.

These modifications are expected to result in a reduction of refrigeration required by over 100 W.

We are studying and plan to run some tests, as required, on the feasibility of changes to the fill system.

Fig. 1.   The sandwich turns.

SEMI-CIRCULAR TOP

BOLTED FLANGE

COIL FACE PLATE

SEALS

COIL DEWAR
INNER WALL

TIE ROD

COIL DEWAR
OUTER WALL

7' DIA.

BRIDGE

BRIDGE

BEAM
CENTERLINE

BOLTED FLANGE

COIL BOTTOM PLATE

DEWAR BOTTOM PLATE

DEWAR SUPPORT LEG

SEALS

MAIN SUPPORT LEG
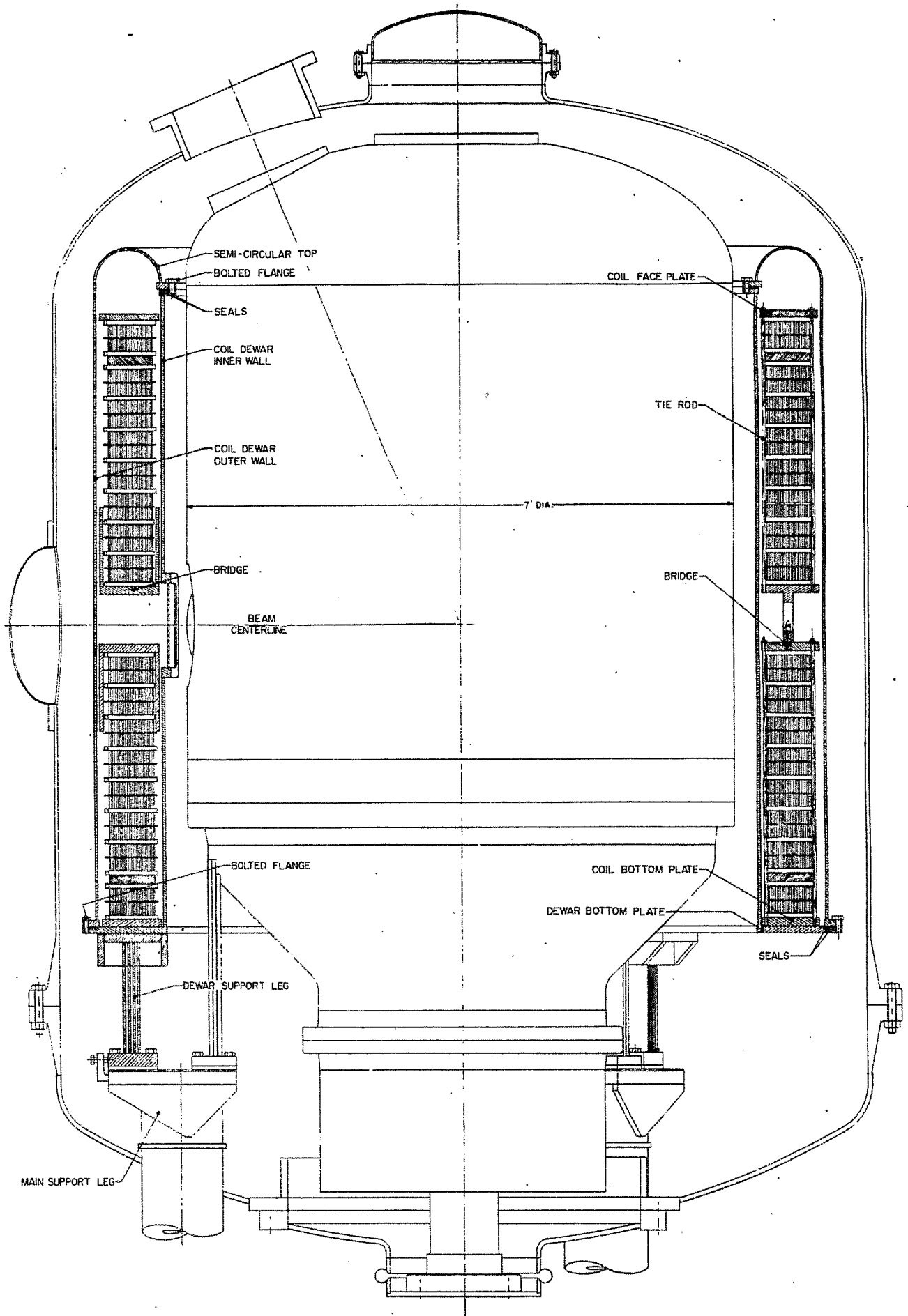
Fig. 2.   Chamber over-all.
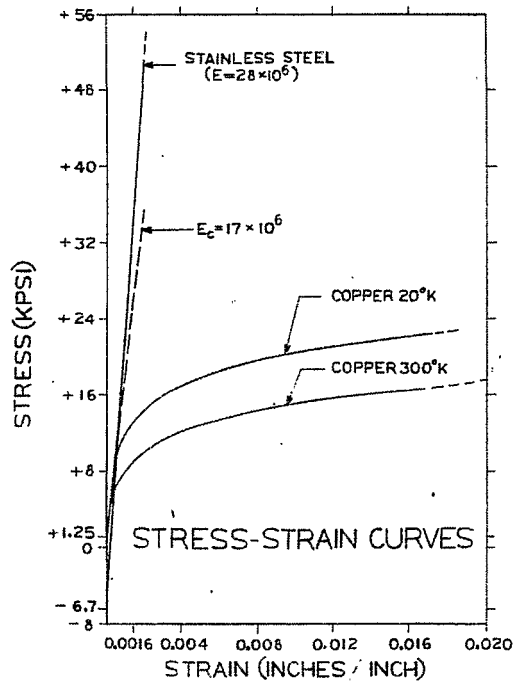
Fig. 3.   Stress-strain, stainless steel-copper.
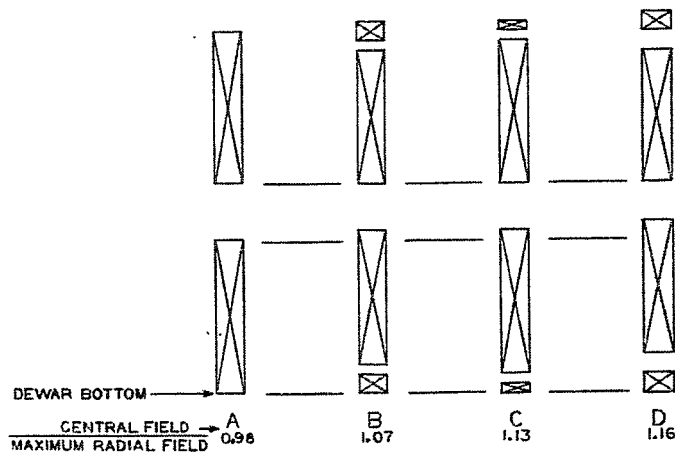
Fig. 4.   Configurations considered, 7 ft magnet.
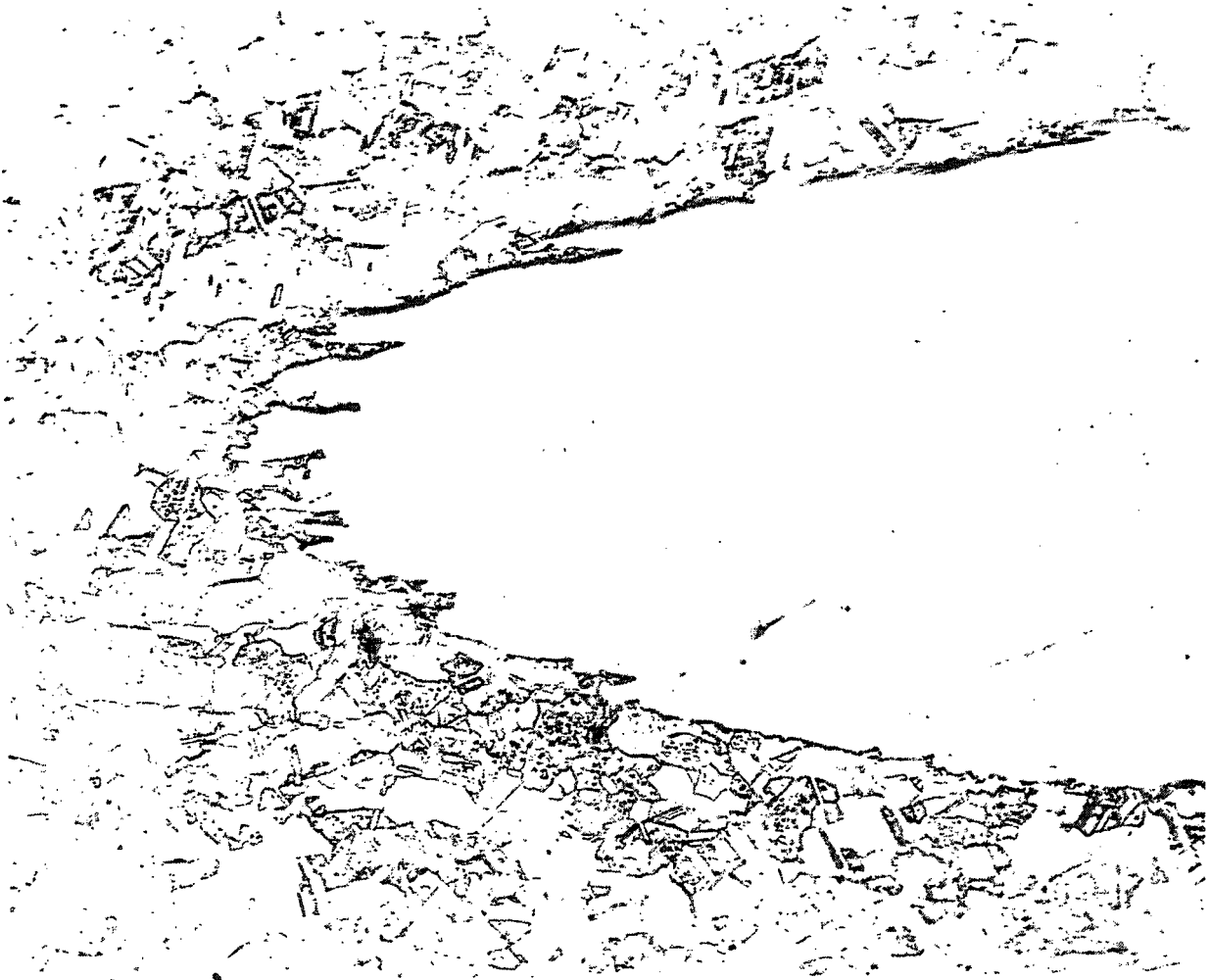
Fig. 5. Photomicrograph of NbTi core in Cu.
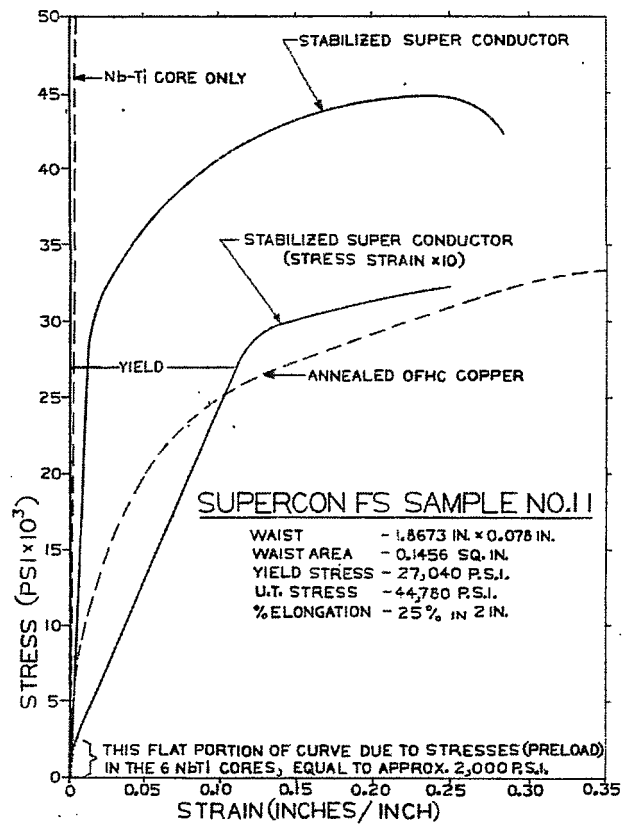
Fig. 6.   Stress-strain curve of composite superconductor.
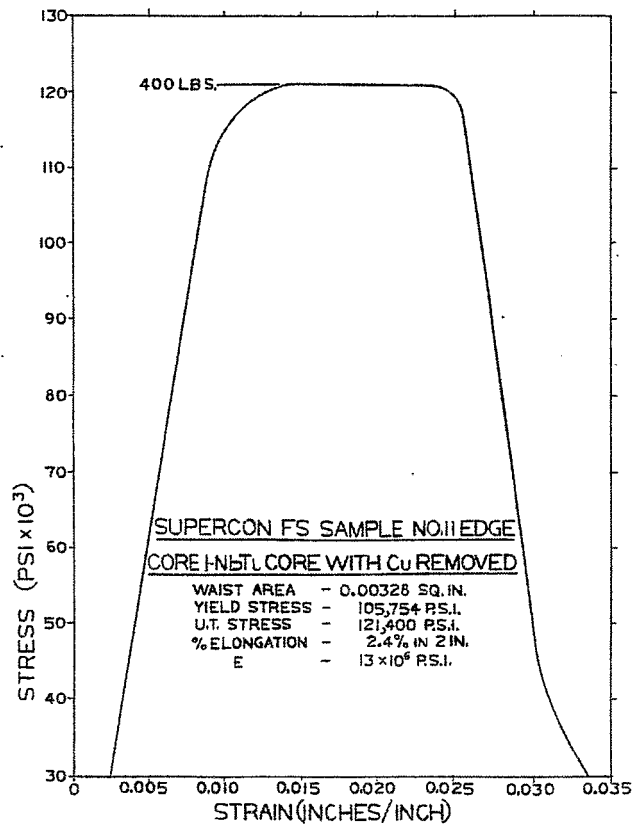
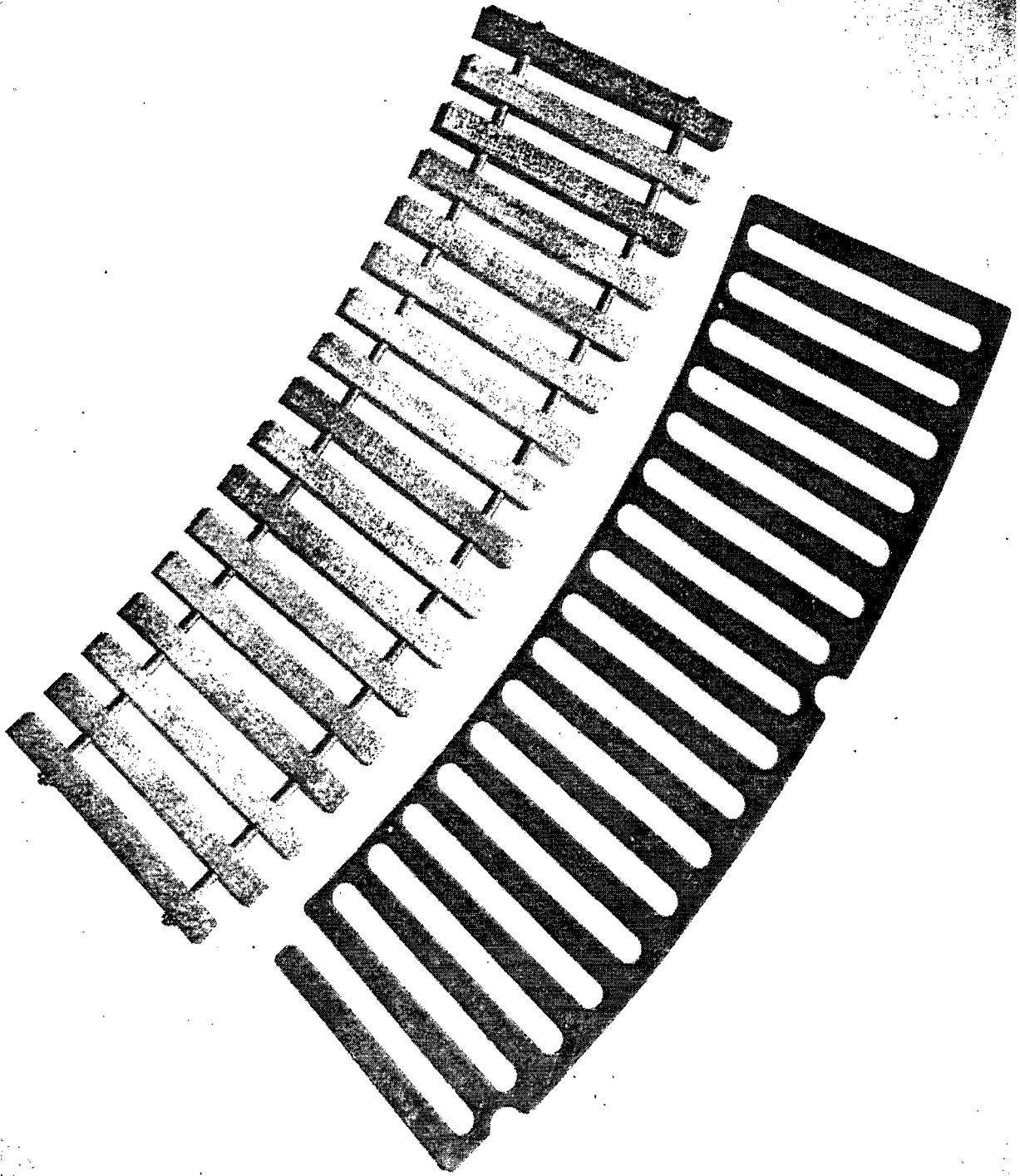Fig. 7.   Stress-strain curve of NbTi superconductor core.

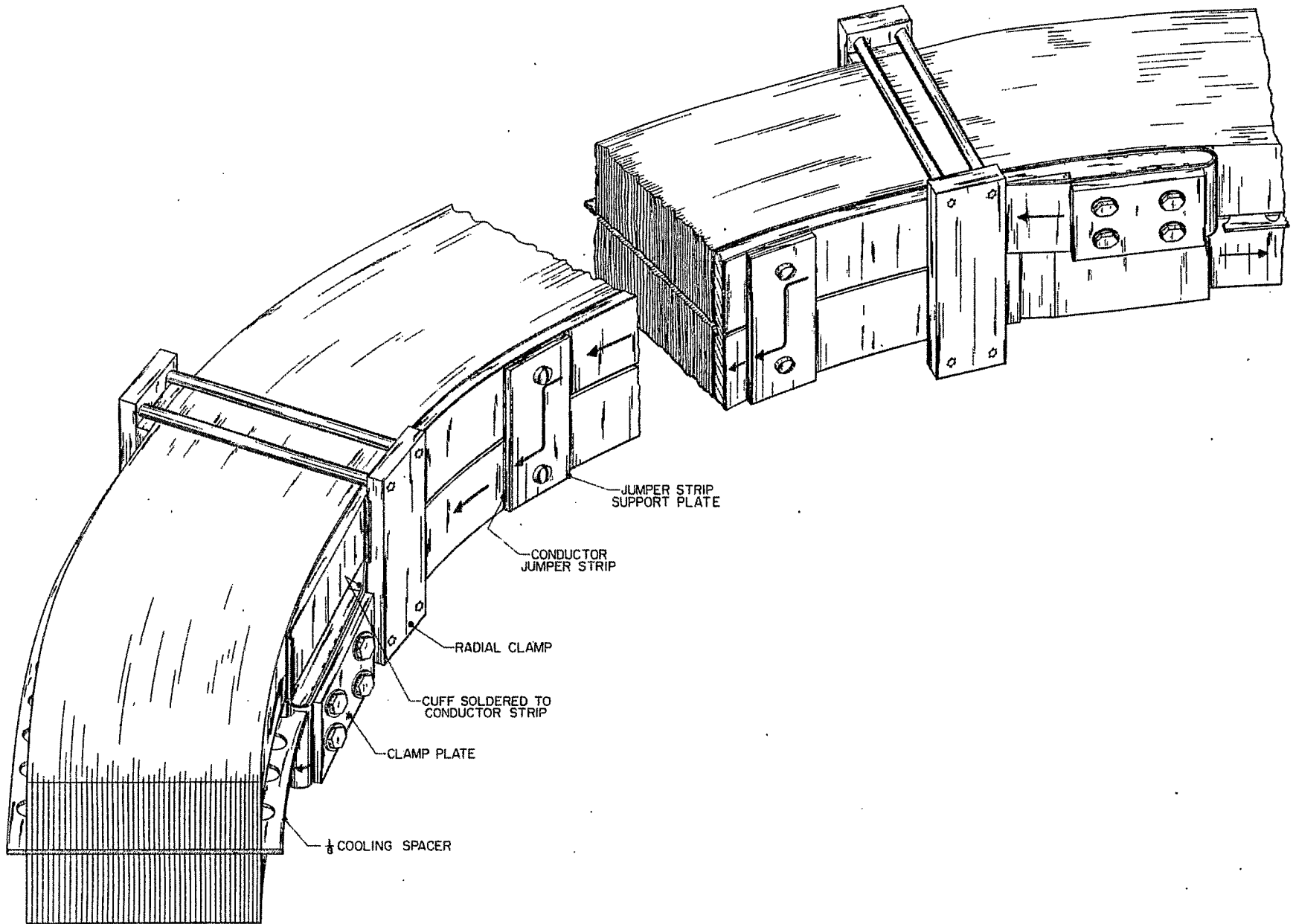Fig. 8.   1/8 in. and 5/8 in. phenolic cooling spacers.

JUMPER STRIP
SUPPORT PLATE

CONDUCTOR
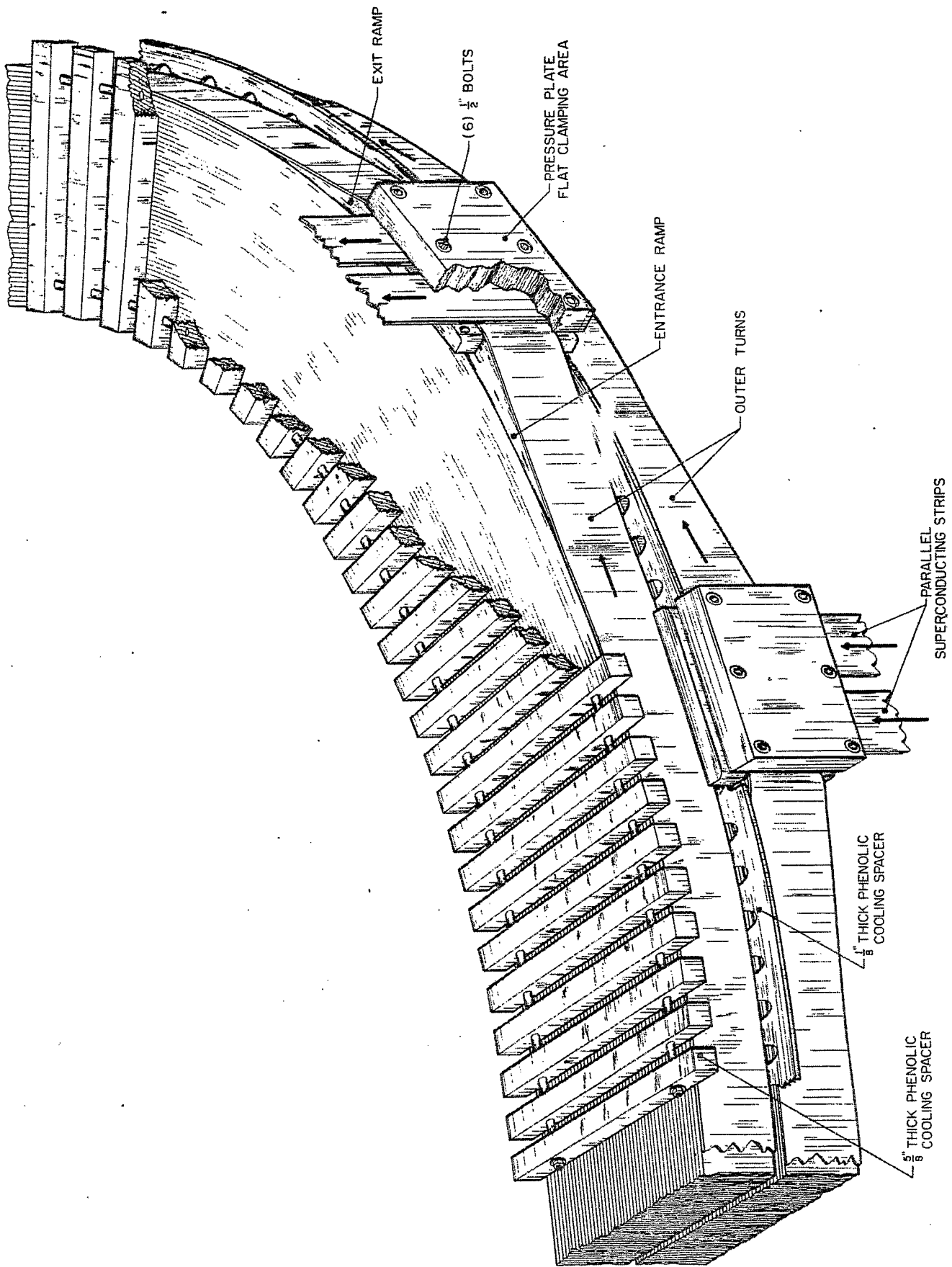JUMPER STRIP

RADIAL CLAMP

CUFF SOLDERED TO
CONDUCTOR STRIP

CLAMP PLATE

$\frac{1}{8}$ COOLING SPACER

Fig. 9. Internal crossover plate assembly.

EXIT RAMP

(6) $\frac{1}{2}$" BOLTS

PRESSURE PLATE
FLAT CLAMPING AREA

ENTRANCE RAMP

OUTER TURNS

PARALLEL
SUPERCONDUCTING STRIPS

$\frac{1}{8}$" THICK PHENOLIC
COOLING SPACER

$\frac{5}{8}$" THICK PHENOLIC
COOLING SPACER

Fig. 10. Inter-pancake electrical connectors.

RADIAL CLAMP

FIBRE GLASS
CLAMPING BLOCK

(4) $\frac{3}{8}$" SCREWS

PRESSURE PLATE

$\frac{1}{8}$" THICK PHENOLIC
COOLING SPACER

$\frac{5}{8}$" THICK PHENOLIC
COOLING SPACER
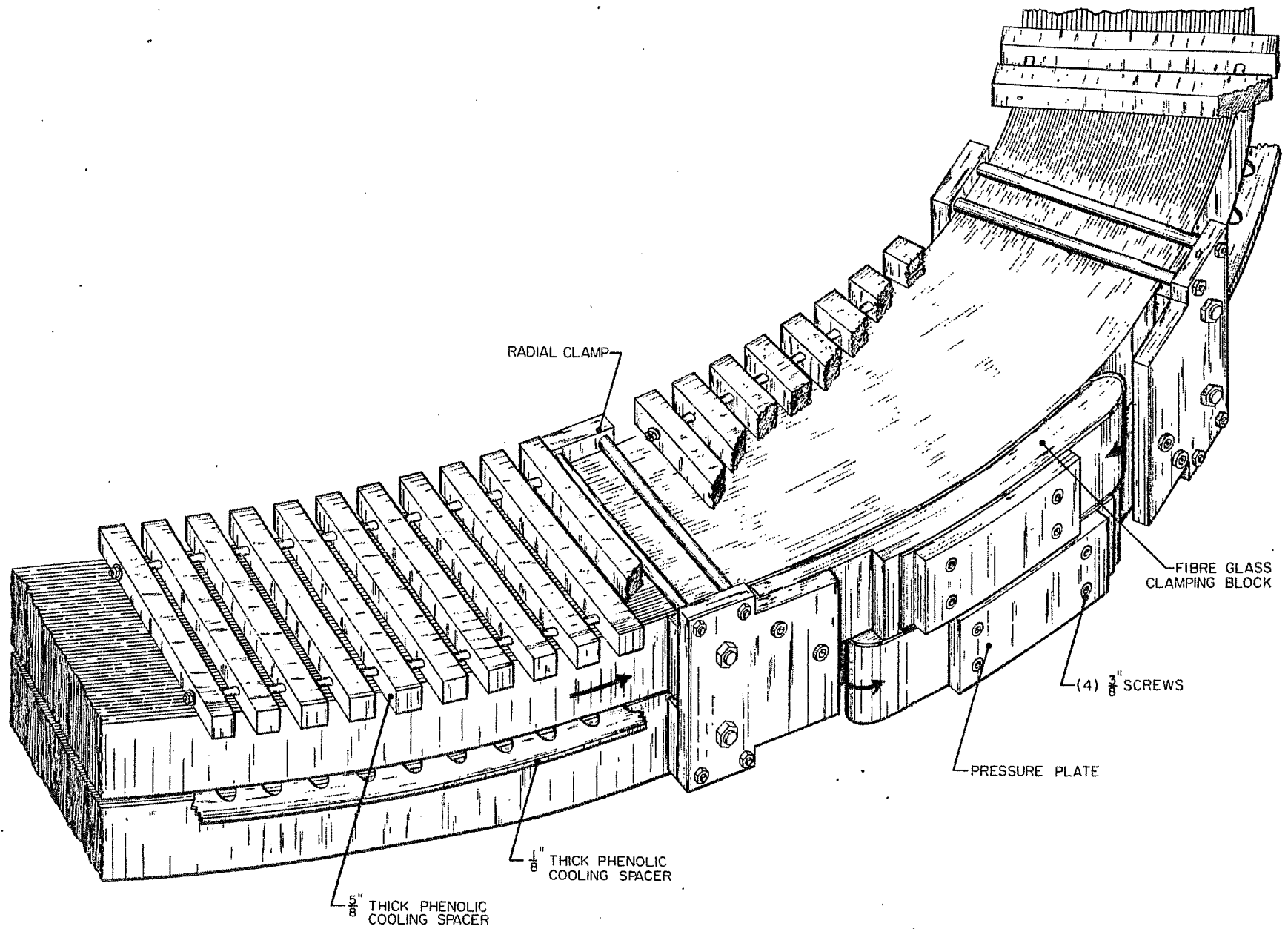
Fig. 11.   End clamp assembly.
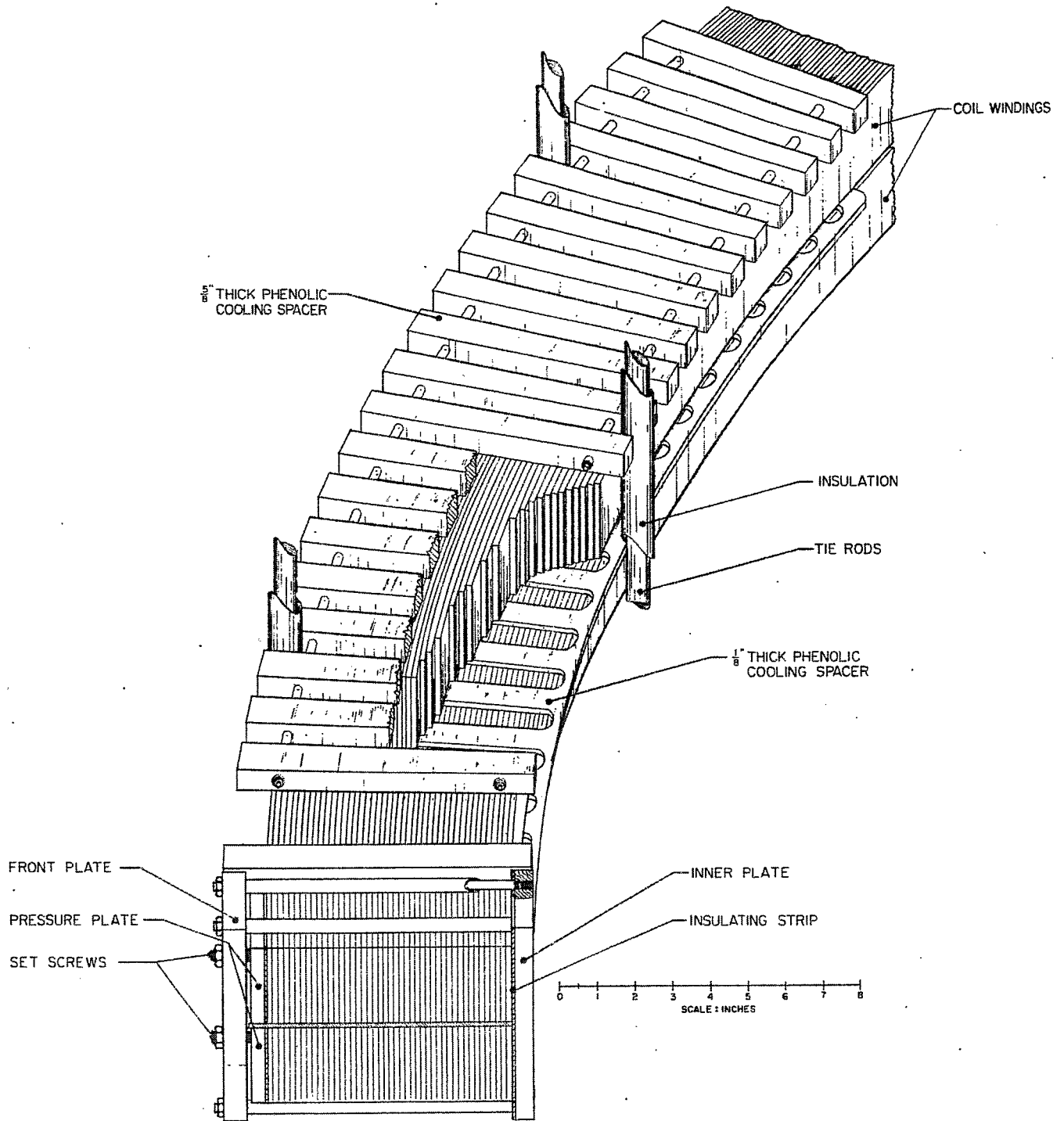
Fig. 12. Radial clamp and cooling spacer details.
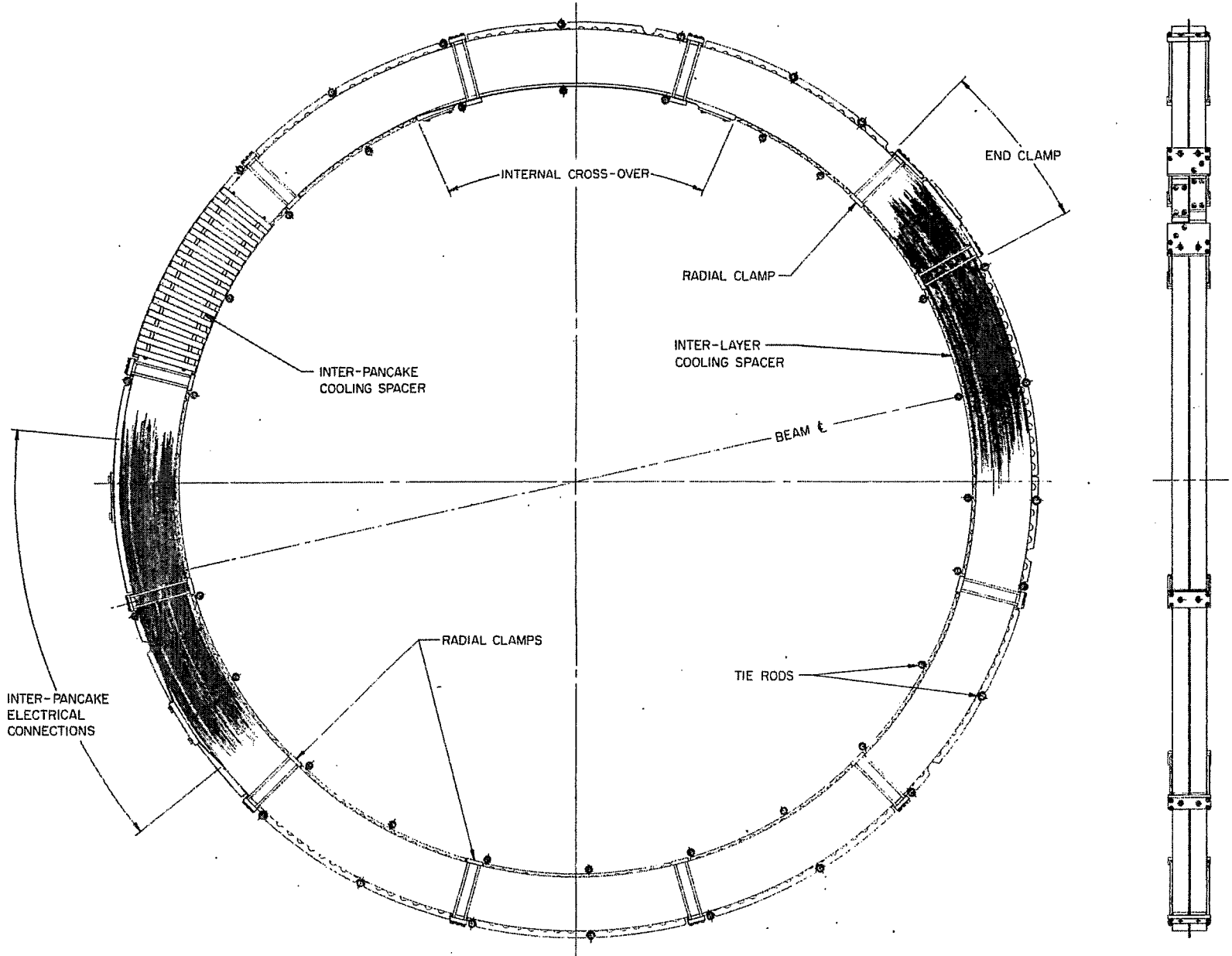
Fig. 13. Plan view of completed pancake.

UPPER COIL
FACE PLATE
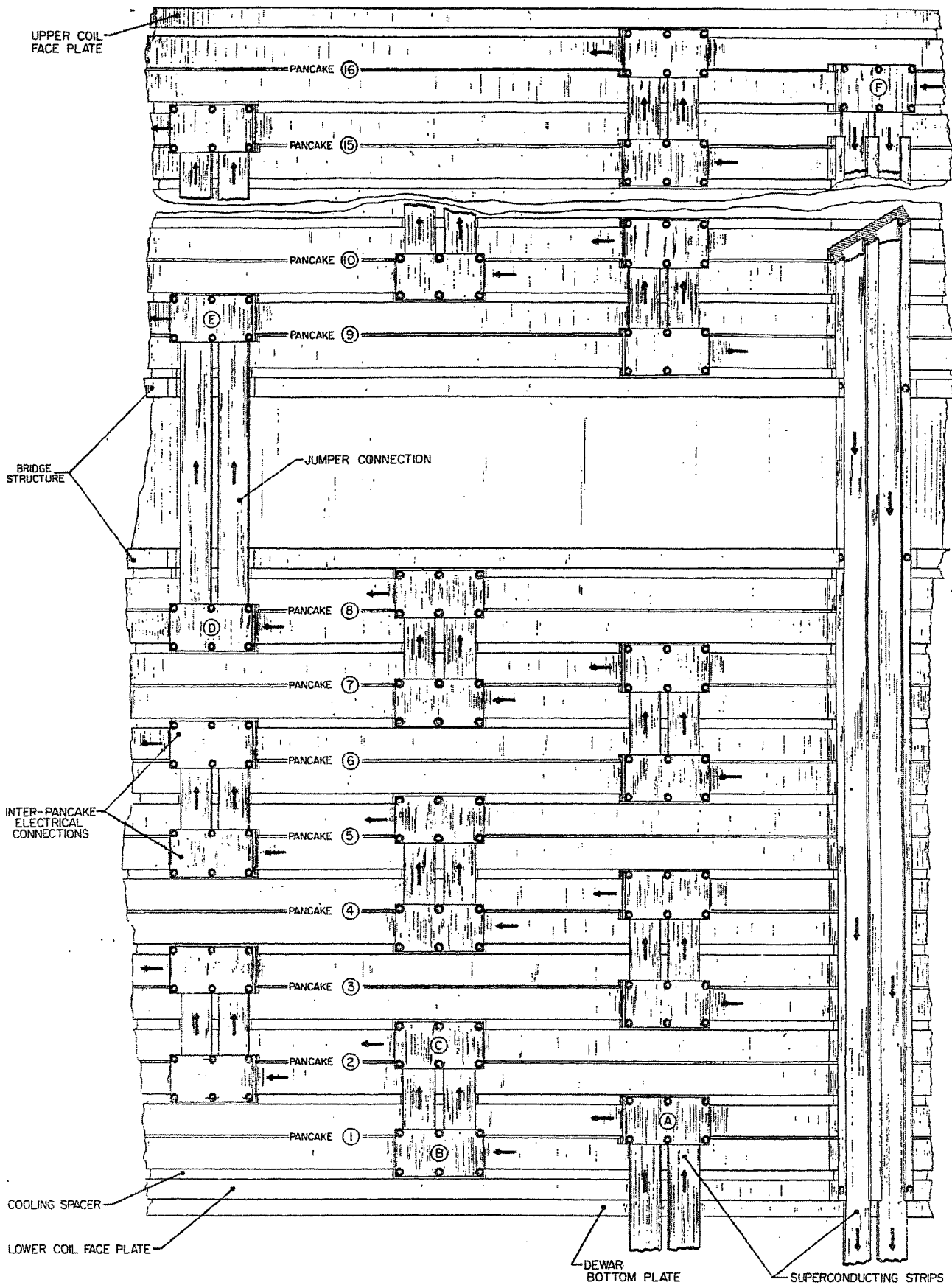
PANCAKE ⑯

PANCAKE ⑮

F

PANCAKE ⑩

E

PANCAKE ⑨

BRIDGE
STRUCTURE

JUMPER CONNECTION

PANCAKE ⑧

D

PANCAKE ⑦

PANCAKE ⑥

INTER-PANCAKE
ELECTRICAL
CONNECTIONS

PANCAKE ⑤

PANCAKE ④

PANCAKE ③

PANCAKE ②

C

PANCAKE ①

B

A

COOLING SPACER

LOWER COIL FACE PLATE

DEWAR
BOTTOM PLATE

SUPERCONDUCTING STRIPS
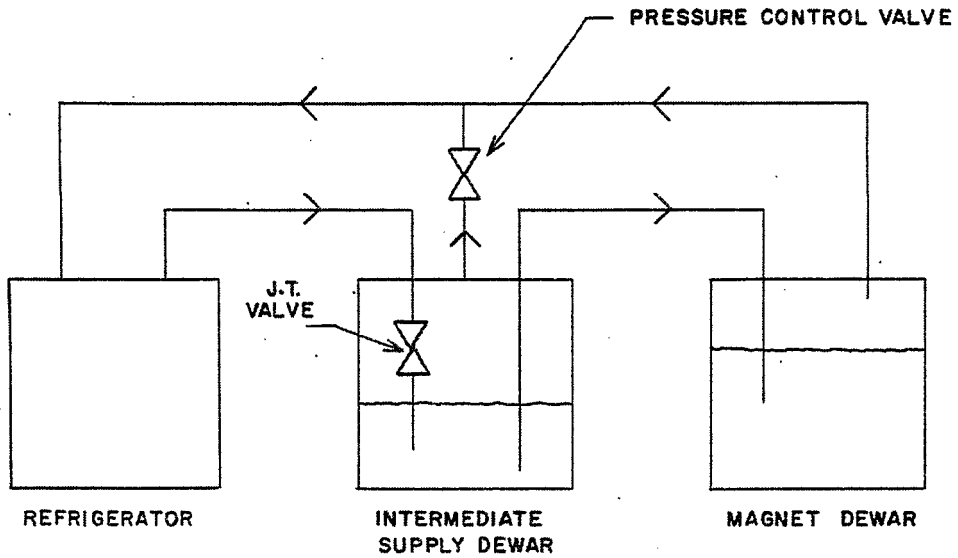
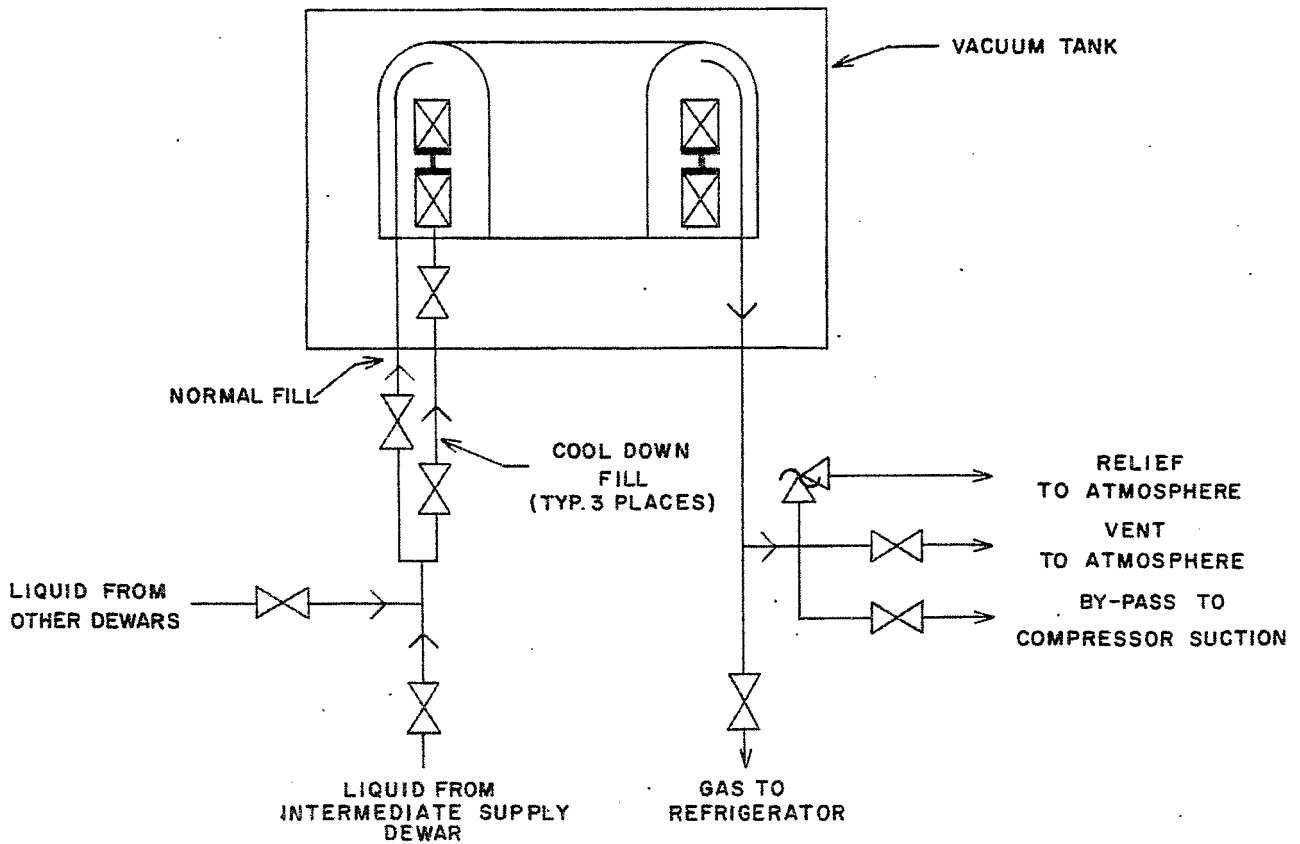Fig. 14. Inter-pancake electrical assembly.

Fig. 15. Simplified refrigerator flow schematic.

Fig. 16. Magnet cooldown and fill system.